

PRECIPITATION OF DISPERSOIDS IN DC-CAST AA3103 ALLOY DURING HEAT TREATMENT

YanJun Li and Lars Arnberg

Department of Materials Technology,
Norwegian University of Science and Technology,
7491, Trondheim, Norway

Abstract

The precipitation behavior of dispersoids in DC cast AA3103 alloy during heating and homogenization at 600°C has been studied by means of TEM, electrical conductivity measurement and image analysis. During heating, α -Al(Mn,Fe)Si is the first phase to precipitate in the alloy. When heated to higher temperature, long rod like and plate like Al_6 (Mn,Fe) dispersoids precipitate in the alloy. During homogenization, the size of Al_6 (Mn,Fe) dispersoids grows while α -Al(Mn,Fe)Si dispersoids dissolve quickly. The evolution of dispersoids during heat treatment is mainly controlled by nucleation, coarsening and dissolution. The size, and number density of dispersoids have been measured. The volume fraction of dispersoids formed during heating, measured from TEM images, has the same trend as the volume fraction calculated from the electrical conductivity of the alloy.

Introduction

Homogenization is a very important thermomechanical process for non heat treatable wrought aluminium alloys. The objectives of homogenization are to eliminate micro segregation, reduce manganese in solid solution and obtain desirable size and distribution of constituent particles including fine dispersoids and coarse primary particles, which have a strong influence on

the recrystallization kinetics, texture development, grain size and mechanical properties of the alloy [1-3]. In the last decades, many investigations have been done to study the precipitation behavior of dispersoids in pure and commercial Al-Mn alloys. The different phases precipitated in Al-Mn alloys, with addition of different alloying elements Fe, Si and Cu, during heat treatment have been identified by Nes [4], Furrer [5], Goel [6], Hasen [7], et al. The influences of alloying elements on the precipitation behavior in Al-Mn alloy have also been studied. It has been found that Fe and Si promote the precipitation of dispersoids and decrease the solubility of Mn in solid solution [6,8-10]. However, quantitative studies on the precipitation of dispersoids, especially on the volume fraction of dispersoids, have been few. The present authors have quantitatively studied the precipitation behavior of dispersoids in a DC-cast 3003 alloy [11]. A method to measure the volume fraction of dispersoids from TEM images has been proposed, by which the volume fraction of dispersoids can be measured accurately.

In present work, the precipitation behavior of dispersoids in a DC-cast 3103 alloy has been studied. The main difference of present material and the 3003 alloy (containing 0.2 wt% Si) studied by present authors before is that the Si content in present 3103 alloy (0.05 wt%) is much lower. The influence of Si on the precipitation behavior has also been discussed.

Experimental

The material used in this experimental work was a DC cast 3103 rolling ingot. The chemical composition of the alloy was (wt%): Mn 1.02, Fe 0.54, Si 0.05, Cu 0.002 and Al bal. Samples were taken from the center locations of the ingot. Heat treatment was conducted in an air circulation furnace with a temperature accuracy of ±2K. Samples were heated to 600°C with heating rate of 50K/h, and then held at this temperature for 24 hours. The samples were quenched into water at different temperatures during heating and after different times of homogenization. The electrical conductivity of the samples was measured at room temperature. TEM foils were prepared by electropolishing in an electrolyte containing two parts methanol and one part nitric acid at -20 °C. Foils were observed in a JEOL 2010 TEM at 200kv. EDS attached to the TEM was used to measure the composition of dispersoids. A GIF system was used to get electron energy lose spectrum, EELS, in order to measure the thickness of the foil for each TEM image. In order to measure the area fraction of precipitate free zone (PFZ), the samples were deep etched with a solution of 10% H₃PO₄ before optical micrographs were taken. Characteristic size parameters of dispersoids and area fraction of PFZ were measured using the image analysis software KS300.

Results and discussion

Solidification structure

The average secondary dendrite arm spacing (SDAS) of the material is about 50 μm. The solidification structure is shown in Fig. 1(a). There is a large fraction of plate like eutectic primary particles distributed on the grain boundaries and in the interdendritic areas. Fig. 1(b) shows the concentration profiles of alloying elements Mn and Fe across the dendrite arm shown in Fig. 1(a). As can be seen, most of the Mn in the alloy exists in the solid solution after solidification, while the concentrations of Fe in the solid solution is very low. The distribution of Mn in the dendrite arms shows a strong segregation. The Mn concentration is much lower in the center and periphery areas of the dendrite arms.

The primary particles have been determined by TEM diffraction pattern and microprobe composition measurement to be orthorhombic Al₆(Mn,Fe) phase. A typical composition of the particles is, in wt.%: Fe 18.02, Mn 6.54, Cu 2.12, Si 0.07, and Al bal. It is interesting to note that there is more than 2wt% Cu in the primary Al₆(Mn,Fe) particles. No α-Al(Mn,Fe)Si particle

has been found in this alloy. This is due to the low content of Si in the alloy. It is well known that Si favors the formation of a-Al(Mn,Fe)Si particles in Al-Mn alloys.

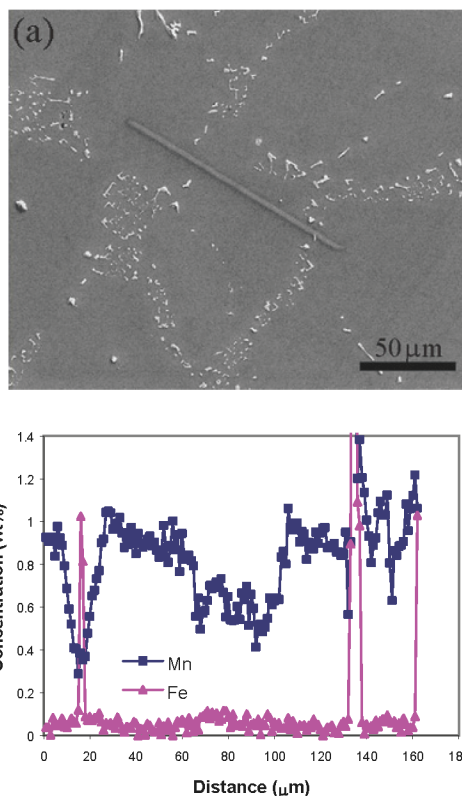


Fig. 1 Solidification structure of 3103 alloy (a) and concentration profiles of Mn and Fe in the dendrite along the track shown in (a).

Electrical conductivity evolution during heat treatment

According to Altenphol [12] and Trømborg [13] the electrical conductivity, EC, of Al-Mn alloys has such a relationship with the concentrations of alloying elements in solid solution

$$\frac{1}{EC} = 0.0267 + 0.032Fe_{ss}\% + 0.033Mn_{ss}\% + 0.0068Si_{ss}\% \quad (1)$$

where, Fe_{ss}%, Mn_{ss}%, Si_{ss}% and Cu_{ss}% are weight percent of Fe, Mn, Si, and Cu, respectively, in solid solution. Since the concentrations of Fe, Si and Cu in solid solution are very low and change little during heat treatment, the electrical conductivity of the alloys can give a detailed indication on the evolution of Mn content in the solid solution.

Fig. 2 shows the electrical conductivity evolution during heat treatment. When the alloy is heated to 350 °C, the EC starts to increase with increasing temperature, indicating that the supersaturated solid solution starts to decompose. The EC of the alloy gets a maximum at about 500 ~530 °C. Then it decreases

with increasing temperature, which indicates the increasing of Mn content in the solid solution with increasing temperature. This is due to the dissolution of dispersoids caused by the increase of solubility of Mn in solid solution. During homogenization at 600 °C, the EC increases with holding time.

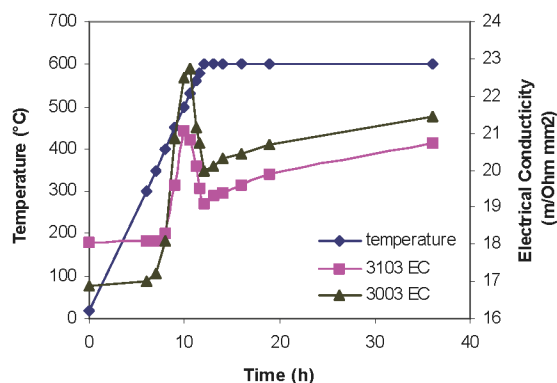


Fig. 2 Evolution of electrical conductivity in the 3103 and 3003[14] alloys during heat treatment.

As a comparison, the EC evolution curve of 3003 alloy is also shown in Fig. 2. It can be seen that the decomposition of the supersaturated solid solution in 3103 alloy is sluggish, and the variation of Mn contents in solid solution during heat treatment in 3103 alloy is less than the 3003 alloy. This result demonstrates the influence of Si to promote the decomposition of supersaturated solid solution and decrease the solubility of Mn in solid solution in Al-Mn alloys.

Precipitation of dispersoids during heating

When the alloy is heated to 350 °C, some very fine dispersoids can be observed in the alloy. This observation is in agreement with the EC curve. The morphology of the dispersoids precipitated during heat treatment is shown in Fig. 3. At the beginning of precipitation, the dispersoids are nearly cubic shaped. With increasing temperature, the dispersoids develops into rectangular parallelepipedic and plate-like shapes. It can be seen from Fig. 3a, most of the dispersoids locate on the dislocations, indicating that dislocations have acted as the nucleation sites for the dispersoids. All the dispersoids precipitated during heating from 350 °C to 580 °C have been determined to be simple cubic α -Al(Mn,Fe)Si phase. The composition of the α dispersoids measured by EDS attached to the TEM shows that the dispersoids has the constitution about $Al_{12-14}(Mn,Fe)_3Si$. The Mn content is much higher than the Fe content in the dispersoids. The Mn/Fe mass ratio of the dispersoids in the samples heated to 500 °C is about 15. The

Mn/Fe ratio decreases with increasing temperature. When the alloy is heated to 600 °C, the Mn/Fe ratio is about 8.

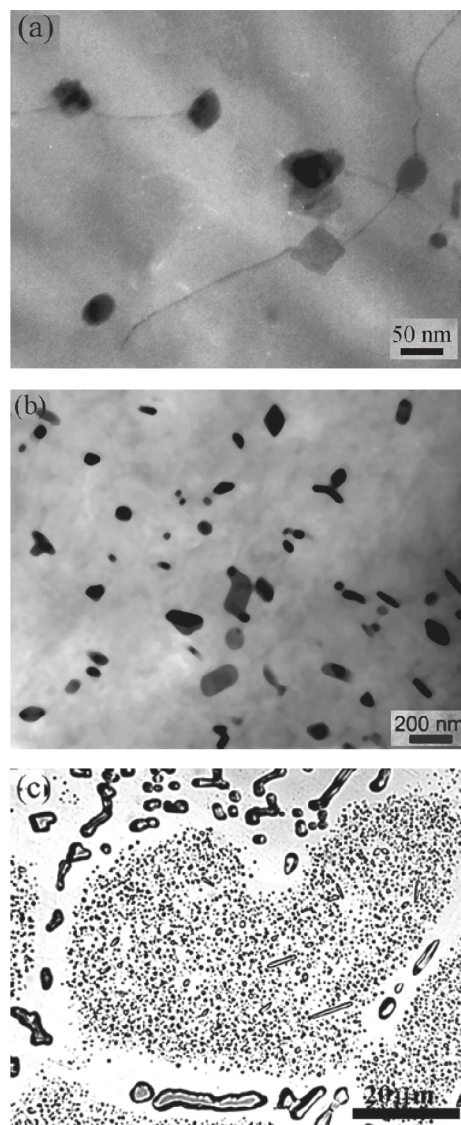


Fig. 3 Morphology of dispersoids precipitated during heating (a) 400 °C, (b) 580 °C and (c) 600 °C

When the alloy is heated to 600 °C, some large plate like and long rod like dispersoids form among the α -Al(Mn,Fe)Si dispersoids, as shown in Fig. 3(c). These dispersoids have been determined to be an orthorhombic $Al_6(Mn,Fe)$ phase. The morphology and diffraction pattern of the $Al_6(Mn,Fe)$ dispersoids are shown in Fig. 4. A large strain field around the plate like dispersoid can be observed. It can be seen from the diffraction pattern that the $Al_6(Mn,Fe)$ dispersoids are semicoherent with the matrix. The orientation relationship between the precipitates and the Al lattice is found to be

$[110]_{Al_6(Mn,Fe)} // [112]_{Al}$ and $[001]_{Al_6(Mn,Fe)} // [\bar{1}3\bar{5}]_{Al}$. $[110]$ is the preferential growth direction of $Al_6(Mn,Fe)$. The large strain fields around these dispersoids are due to the semicoherence between the dispersoids and matrix.

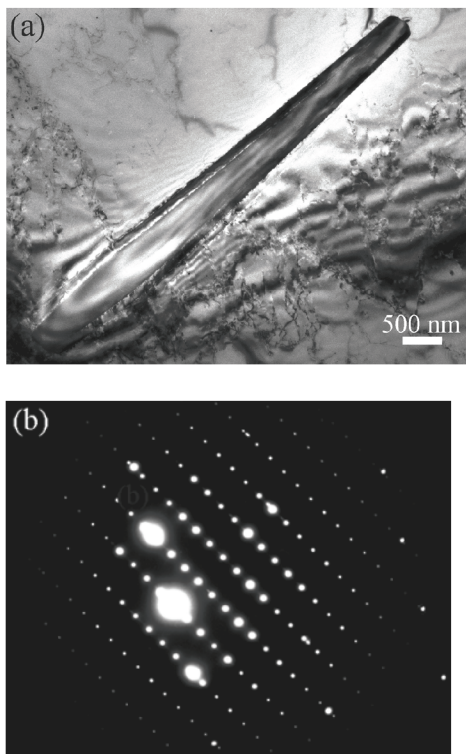


Fig. 4 Morphology of the plate like $Al_6(Mn,Fe)$ dispersoid (a) and the corresponding electron diffraction pattern (b). In the diffraction pattern, the electron beam is parallel to $[112]_{Al}$ and $[110]_{Al_6(Mn,Fe)}$

Fig. 5 shows the size evolution of dispersoids during heat treatment. The size of dispersoids grows continuously with heating temperature. The number density of α dispersoids in the alloy during heat treatment is shown in Table 1, in which the number density is only measured in the grains with dispersoids densely populated. As can be seen, the number density decreases with heating temperature and holding time during homogenization. It indicates that the size growth of dispersoids during heat treatment is mainly controlled by the coarsening. When the alloy is heated to higher temperatures than 500 °C, there is also dissolution of dispersoids caused by the increase of Mn solubility in solid solution. By comparing the minimum ferret diameter, F_{min} and maximum ferret diameter, F_{max} , of dispersoids, it can be seen that the average aspect ratio of dispersoids decreases with heating temperature during heating.

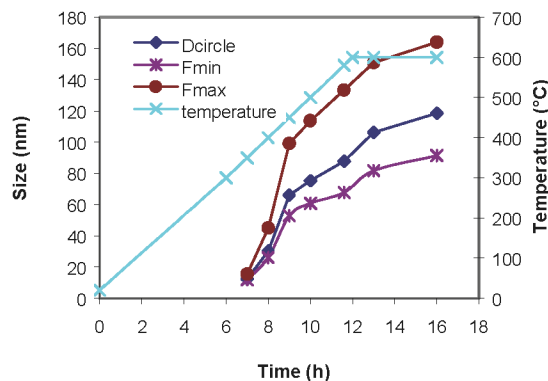


Fig. 5 Size evolution of the α - $Al(Mn,Fe)Si$ dispersoids precipitated during heat treatment

As a comparison, the number density of dispersoids precipitated in AA3003 alloy during heat treatment is also shown in Table 1. The number density of dispersoids precipitated in 3103 alloy at low temperatures is much less than in the 3003 alloy. It demonstrates that Si has also the influence to promote the nucleation of dispersoids in Al-Mn alloys.

Table 1 Number density of α - $Al(Mn,Fe)Si$ dispersoids precipitated during heat treatment (μm^{-3})

Alloy	400 °C	500 °C	580 °C	600 °C, 1h	600 °C, 4h
3103	305	101	22	13	5
3003 ^[14]	1495	306	70	26	9

The spatial distribution of dispersoids in the matrix can be seen from the light optical microscope images shown in Fig. 6. At low temperatures, the dispersoids distribute inhomogeneously in dendrite arms, especially in the coarse dendrite arms. Except for a large fraction of precipitate free zones on the grain boundaries and interdendritic areas, the population of dispersoids in the center of the coarse dendrite arms is very sparse. This is because these areas are Mn depleted in solid solution, which cause the late decomposition of the supersaturated solid solution and less precipitation of Mn from the matrix. With increasing temperature, more Mn precipitates from the solid solution, thus the number density of dispersoids in the center of dispersoids increases. As can be seen from Fig.6 (b), the distribution of dispersoids in the grains becomes more homogeneous when the alloy is heated to 500 °C. However, when the alloy is heated to higher temperatures, the population of dispersoids in the center of coarse dendrite arms becomes sparse again, as shown in Fig.6 (c). This is because the dissolution of dispersoids, which is caused by the increase of

solubility of Mn in solid solution, within the Mn-depleted areas has more driving force.

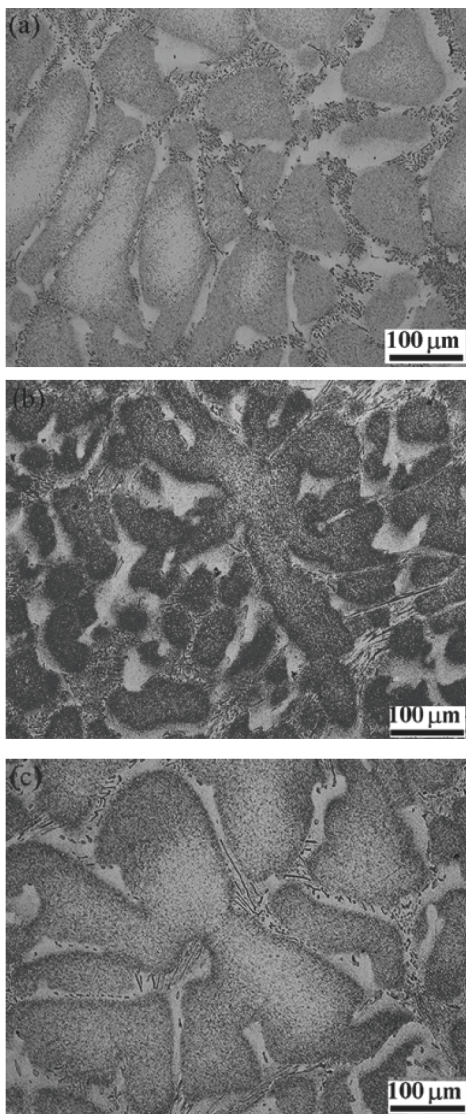


Fig. 6 Spatial distribution of dispersoids during heating (50 °C/h) (a) 450°C, (b) 500 °C and (c) 580 °C.

Precipitation of dispersoids during homogenization

Fig. 7 shows the morphology and spatial distribution of dispersoids in the alloy after homogenization at 600 °C. The long rod like $Al_6(Mn,Fe)$ dispersoids grow quickly while $\alpha-Al(Mn,Fe)Si$ dispersoids dissolves quickly during homogenization. After 7h of homogenization, there are only a few $\alpha-Al(Mn,Fe)Si$ dispersoids left within some grains in the alloy. The size and number density of $\alpha-Al(Mn,Fe)Si$ dispersoids have been shown in Tab.1 and Fig. 5. The size growth of the $\alpha-Al(Mn,Fe)Si$ dispersoids is due to the coarsening between the dispersoids. The quick dissolution of α dispersoids in the alloy is due to the low Si content in the

matrix, which makes α -dispersoids become a thermodynamically unstable phase at high temperature. Therefore, the $Al_6(Mn,Fe)$ dispersoids grow quickly at the expense of the surrounding α dispersoids. The size evolution of $Al_6(Mn,Fe)$ dispersoids is also controlled by the coarsening between the dispersoids. As can be observed in Fig. 7(b), the size of dispersoids has grown much while the population of the dispersoids has dropped much after 24h of homogenization.

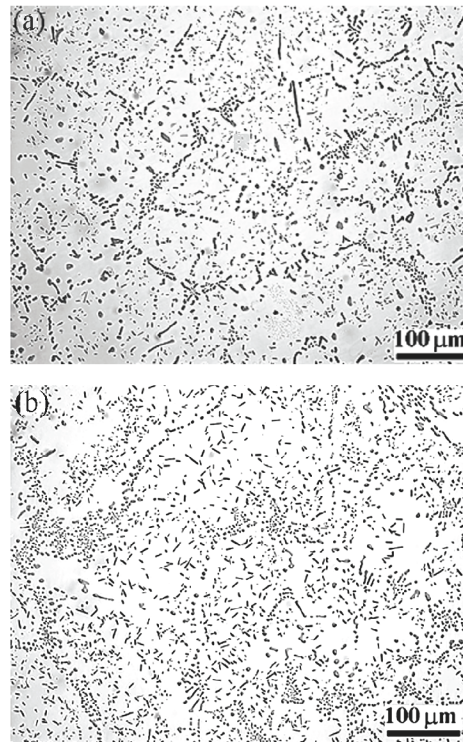


Fig. 7 Morphology of dispersoids in 3103 after homogenization at 600°C for (a) 7h and (b) 24h.

PFZ evolution during heat treatment

It has been shown in Fig. 6 that there is a large fraction of PFZ in the alloy during heat treatment. Fig. 8 shows the evolution of area fraction of precipitate free zones, A_{PFZ} , during heat treatment. During heating, the A_{PFZ} decrease with heating temperature. At about 500 °C ~530°C, the A_{PFZ} gets the minimum. Then it grows with increasing temperature. As can be observed in Fig. 6 and Fig. 7, all the PFZ locates in the Mn-depleted areas formed during solidification. It suggests that the PFZ is originated from the Mn segregation in the alloy. Since the content of Mn in α dispersoids is much higher than Fe and Si, and the diffusion constants of Si and Fe in aluminium are all higher than Mn, the evolution of PFZ is controlled by the concentration and solubility of Mn in the solid solution. At the

beginning of the precipitation of dispersoids, there are no dispersoids in the Mn-depleted areas. Thus the A_{PFZ} is very high. With increasing temperature, more and more Mn precipitates from the solid solution, hence the precipitation of dispersoids extends slowly to the Mn-depleted areas. Therefore, the A_{PFZ} decreases with heating temperature. When the alloy is heated to high temperature, the dispersoids in the Mn-depleted areas will dissolve due to the solubility increase of Mn in solid solution. At the same time, the coarsening between the Mn-rich dispersoids and Fe-rich primary particles can also cause the dissolution of the dispersoids surrounding the primary particles. As a result, the A_{PFZ} increases with heating temperature. The increase of A_{PFZ} with holding time at the beginning of homogenization is also due to the coarsening process between the dispersoids and primary particles. But, after 4h of homogenization, the A_{PFZ} is difficult to measure in the alloy due to the growth of long rod like $Al_6(Mn,Fe)$ into the PFZ areas. After 7 h of homogenization at 600 °C, there is nearly no PFZ in the alloy. This result shows that the precipitation of long rod like $Al_6(Mn,Fe)$ dispersoids has the influence to promote the homogeneity of the distribution of dispersoids in the alloy.

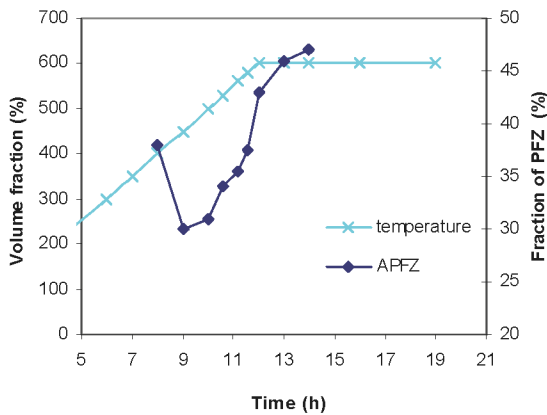


Fig. 8 Area fraction of PFZ during heat treatment

Volume fraction of dispersoids

The present authors have proposed a method to measure the volume fraction, V_v , of rectangular parallelepipedic dispersoids from TEM images by equation [11]

$$V_v = A_A \frac{\bar{K} \bar{D}}{\bar{K} \bar{D} + t} \cdot (1 - A_{PFZ}) \quad (2)$$

Where \bar{D} and A_A are, respectively, the average equivalent diameter and area fraction of in TEM image; t is the thickness of TEM specimen, \bar{K} is the average shape factor of dispersoids in the alloy. For a rectangular parallelepipedic dispersoid with

length a , width b and height c , its shape factor K can be calculated by

$$K = \frac{\sqrt{2\pi k_1 k_2}}{[k_1 + k_2 + k_1 k_2]^{1/2}} \quad (3)$$

where, $k_1=b/a$, $k_2=c/a$. The volume fraction of dispersoids precipitated during heat treatment measured from TEM images is shown in Fig. 9. Due to the difficulty to measure the number density of long rod like $Al_6(Mn,Fe)$ dispersoid by TEM, the volume fraction of dispersoids after 7h of homogenization is not measured.

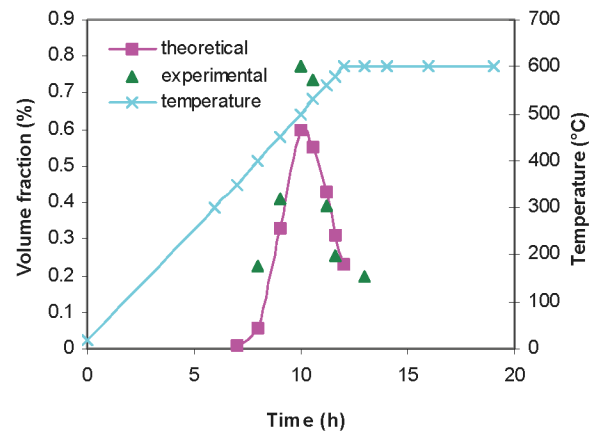


Fig. 9 Volume fraction of α -Al(Mn,Fe)Si dispersoids during heat treatment

If we assume the variation of Mn and Fe in solid solution during heating is only resulted by the dissolution and precipitation of dispersoids, the volume fraction of the dispersoids in the alloy can be calculated by the EC evolution. According to equation (1) the concentration change of (Fe+Mn) in solid solution, in wt.%, can be calculated by

$$\Delta(Fe + Mn)_{ss} = \frac{1}{0.033} \left[\frac{1}{EC(T)} - \frac{1}{EC(0)} \right] \quad (4)$$

where, $EC(0)$ and $EC(T)$ are, respectively, room temperature electrical conductivity of the alloy before heat treatment and after quenched from temperature T. In the present work the constitution of the α dispersoids is assumed to be $Al_{12}(Mn,Fe)_3Si$. The calculated volume fraction of dispersoids during heating is also shown in Fig. 9. As can be seen, the measured and the calculated volume fraction have the same trend during heating. However, the measured volume fraction of dispersoids is higher than the calculated volume fraction at low temperatures. This is due to the inhomogeneous distribution of dispersoids in the alloy. The size and number density of dispersoids have only been measured in those grains with

dispersoids densely distributed. At higher temperatures, the measured volume fraction of dispersoids is slightly lower than the calculated one. This is due to the coarsening between the coarse primary particles and dispersoids, which makes the primary particles grow by the expense of the dispersoids.

Conclusions

The supersaturated solid solution of the 3103 alloy starts to decompose at about 350 °C by the precipitation of simple cubic α -Al(Mn,Fe)Si dispersoids. Due to the segregation of Mn in dendrite arms during solidification, the distribution of dispersoids in grains is inhomogeneous. The population of dispersoids in the center of coarse dendrite arms is sparse.

Due to the low Si content in the alloy, the decomposition of the supersaturated solid solution is sluggish and the number density of dispersoids is low. The low Si content in the alloy makes the $\text{Al}_6(\text{Mn,Fe})$ dispersoids a stable phase at high temperature.

The size of dispersoids increases with heating temperature and holding time during homogenization. The size evolution of dispersoids is mainly controlled by coarsening during heating. During homogenization at 600 °C, the α dispersoids dissolve quickly into the matrix, while the $\text{Al}_6(\text{Mn,Fe})$ dispersoids grow quickly at the expense of the α dispersoids.

The evolution of area fraction of PFZ during heating in the alloy is controlled by the concentration and solubility of Mn in solid solution and the coarsening between the Fe-rich primary particles and their surrounding Mn-rich dispersoids. During homogenization at 600 °C, due to the quick growth of long rod like $\text{Al}_6(\text{Mn,Fe})$ dispersoids, there is no clear PFZ in the alloy, which makes the distribution of dispersoids more homogeneous.

The volume fraction of dispersoids precipitated during heating is measured. The measured volume fraction has the same trend as the calculated volume fraction.

Acknowledgements

This research was carried out as part of the Fifth Framework Competitive and Sustainable Growth program project GRD1-1999-10921 VIRCAST (Contract N° G5RD-CT-2000-00153). It included the partners: Aluisse Technology & Management Ltd., Switzerland, Calcom SA, Switzerland, Elkem Aluminum ANS, Norway, École Polytechnique Fédérale de Lausanne, Switzerland, Hoogovens Corporate Services, The Netherlands,

Hydro Aluminum AS, Norway, Institute National Polytechnique de Grenoble, France, Institute National Polytechnique de Lorraine, France, Norwegian University of Science and Technology, Norway, Péchiney S.A., France, VAW aluminum AG, Germany, and IFE, Norway and SINTEF, Norway, as major subcontractors. Funding by the European Community and by the Office Fédéral de l'Éducation et de la Science (Bern) for the Swiss partners is gratefully acknowledged. The present authors would like to thank A. L. Dons for her valuable discussion.

References

- [1] E. Nes, "The Effect of a Fine Particle Dispersion on Heterogeneous Recrystallization," *Acta Metallurgica*, 24 (1976), 391.
- [2] F. J. Humphreys, "The Nucleation of Recrystallization at Second Phase Particles in Deformed Aluminium," *Acta Metallurgica*, 25 (1977), 1323-1344.
- [3] Y. Kwag and J. G. Morris, "The effect of structure on the Mechanical Behavior and Stretch Formability of Constitutionally Dynamic 3000 Series Aluminum Alloys," *Materials Science and Engineering*, 77 (1986), 59-74.
- [4] E. Nes, S.E. Naess and R. Hoier, "Decomposition of an Aluminium-Manganese Alloy," *Z. Metallkde.*, 63 (1972), 248-253.
- [5] P. Furrer, "Gefügeänderungen bei der Wärmebehandlung von Al-Mn-Stranggüßbarren," *Z. Metallkde.*, 70 (11) (1979), 699-706.
- [6] D.B. Goel, P. Furrer, and H. Warlimont, "Ausscheidungsverhalten von Aluminium- Mangan-(Kupfer,-Eisen-) Legierungen," *Aluminium*, 8(1974), 511-516.
- [7] V. Hansen, J. Gjønnes, and B. Andersson, "Quasicrystal as Part of the Precipitation Sequence in an Industrial Cast Aluminium Alloy," *J. Mater. Sci. Lett.*, 8(1989), 823- 826.
- [8] P.C.M. Haan, J.V. Rgkom, J. A. H. Sontgerath, "The precipitation Behaviour of High-Purity Al-Mn Alloys," *Materials Science Forum*, vols. 217-222(1996), 765-770
- [9] G. Hausch, P. Furrer, and H. Warlimont, "Crystallisation and Precipitation in Al-Mn-Si alloys," *Z. Metallkde.*, 69(1978), 174.
- [10] P. Kolby, C. Sigli, and C.J. Simensen, "Solubility Limit of Mn and Si in Al-MnSi at 550°C," *Proceedings of the 4th International Conference on Aluminium alloys: their Physical and Mechanical Properties*, ed. L. Arnberg, et al. (Trondheim, 1994), 508-512.
- [11] Y.J. Li and L. Arnberg, "Quantitative Study on the Precipitation of Dispersoids in DC-Cast 3003 Alloy During Heating and Homogenization", submitted to *Acta. Mater.*, 2002
- [12] D. Altenpohl, *Aluminium und Aluminiumlegierungen*, (Berlin: Springer Verlag, 1965), 526.
- [13] E. Trømborg, et al., "Computer modelling as a Tool for Understanding the Precipitation of Mn in AA3xxx Alloys", *The 6th Conference on Modeling of Casting, Welding and Advanced Solidification Processes*, ed. T.S Piwonka, V. Voller and L. Katgerman, (TMS, 1993), 101.
- [14] Y.J. Li and L. Arnberg, "Precipitation of Dispersoids in DC-Cast AA3003 Alloy" *Mater. Sci. Forum*, 396-402(2002), 875-880.